Mechanical Properties of Nafion and Titania/Nafion Composite Membranes for Polymer Electrolyte Membrane Fuel Cells

M. BARCLAY SATTERFIELD,[1] PAUL W. MAJSZTRIK,[2] HITOSHI OTA,[2] JAY B. BENZIGER,[1] ANDREW B. BOCARSLY[2]

[1]Department of Chemical Engineering, Princeton University, Princeton, New Jersey 08544

[2]Chemistry Department, Princeton University, Princeton, New Jersey 08544

Received 23 January 2006; revised 21 March 2006; accepted 13 April 2006
DOI: 10.1002/polb.20857
Published online in Wiley InterScience (www.interscience.wiley.com).

ABSTRACT: Measurements of the mechanical and electrical properties of Nafion and Nafion/titania composite membranes in constrained environments are reported. The elastic and plastic deformation of Nafion-based materials decreases with both the temperature and water content. Nafion/titania composites have slightly higher elastic moduli. The composite membranes exhibit less strain hardening than Nafion. Composite membranes also show a reduction in the long-time creep of ~40% in comparison with Nafion. Water uptake is faster in Nafion membranes recast from solution in comparison with extruded Nafion. The addition of 3–20 wt % titania particles has minimal effect on the rate of water uptake. Water sorption by Nafion membranes generates a swelling pressure of ~0.55 MPa in 125-μm membranes. The resistivity of Nafion increases when the membrane is placed under a load. At 23 °C and 100% relative humidity, the resistivity of Nafion increases by ~15% under an applied stress of 7.5 MPa. There is a substantial hysteresis in the membrane resistivity as a function of the applied stress depending on whether the pressure is increasing or decreasing. The results demonstrate how the dynamics of water uptake and loss from membranes are dependent on physical constraints, and these constraints can impact fuel cell performance. © 2006 Wiley Periodicals, Inc. J Polym Sci Part B: Polym Phys 44: 2327–2345, 2006

Keywords: ionomer; mechanical properties; Nafion; PEM fuel cells; polymer composites; structure-property relations; water sorption

INTRODUCTION

Polymer electrolyte membrane (PEM) fuel cells based on perfluorinated membranes have successfully been operated in a temperature range of approximately 50–90 °C.[1–3] Efforts to develop polymer membranes able to operate above 120 °C have been prompted by the additional benefits of enhanced carbon monoxide (CO) tolerance and improved heat removal.[4–8] The most significant barrier to running a polymer electrolyte fuel cell at elevated temperatures is maintaining the proton conductivity of the membrane. Most polymer membranes rely on absorbed water to ionize acid groups and permit proton transport. The conductivity of a dry membrane is several orders of magnitude lower than that of a fully saturated membrane; proton conductivity increases exponentially with water activity in the membrane. Increasing the fuel cell temperature raises the vapor pressure required to keep a given amount of water in the membrane, thereby increasing the likelihood that water loss will occur and significantly reduce proton conductivity.

Correspondence to: J. B. Benziger (E-mail: benziger@princeton.edu)

Journal of Polymer Science: Part B: Polymer Physics, Vol. 44, 2327–2345 (2006)

Water management is a significant challenge for polymer electrolyte fuel cell operation. To keep the membrane fully hydrated, it is essential to increase the pressure in the fuel cell above the water vapor pressure. The other hydration method—operating with fully humidified feeds—creates a situation in which water that has formed in the fuel cell can flood the gas flow channels. However, avoiding flooding by keeping the water activity below unity can dehydrate the membrane and reduce the proton conductivity. In addition, changes in the water activity result in dimensional changes of the polymer as the polymer absorbs water.[9–14] Water sorption creates an internal pressure in the membrane that causes it to swell against the confinement of the electrodes.[15] The amount of water sorption of the membrane is determined by a balance between the membrane swelling pressure and the applied pressure from the electrode pressing against the membrane. In addition, the mechanical properties of the polymer change as functions of the temperature and water content. Further complications can result from taking the polymer above its glass transition (~110 °C for dry protonated Nafion),[16–19] which can cause polymer chain rearrangements, leading to structural changes in the membrane at the molecular scale. These changes in the polymer properties may lower the membrane stability, performance, and lifetime.[20–22]

We have studied the dynamic performance of fuel cell startup from a dry state and the current response to changes in the load. We have observed a multistep change in the current; this suggests that the membrane swells as it absorbs water, which alters the membrane electrode interface. It has also been observed that increasing the applied pressure sealing the fuel cell causes the internal membrane electrode assembly (MEA) resistance to increase, and this has been attributed to the physical confinement of the Nafion membrane in a fuel cell limiting the water absorbed.[15,23]

The addition of an inorganic material to a polymer membrane can alter and improve the physical and chemical polymer properties of interest [e.g., elastic modulus, proton conductivity, solvent permeation rate, tensile strength, hydrophilicity, and glass-transition temperature (T_g)] while retaining the polymer properties important to enabling the operation in the fuel cell. A number of investigators have examined composite membranes for use in polymer electrolyte fuel cells.[7,8,24–35] The composite membranes may also improve the water-retention properties of these membranes under low-humidity conditions. We have examined a number of composite polymer/inorganic membranes (Nafion/zirconium phosphate, Nafion/titania, Nafion/silica, and Nafion/alumina) in fuel cells at elevated temperatures. Little correlation has been found between the fuel cell performance and chemical formulation, and this has led us to suggest that mechanical properties may play an important role in the improved performance of Nafion composite membranes in fuel cells.

Because of the evidence for mechanical properties affecting the water content of a polymer membrane, a program was initiated to measure the physical and mechanical properties of Nafion and Nafion composite membranes, especially under conditions relevant to PEM fuel cell operation (elevated temperature, elevated water activity, and constrained environments). In this article, we describe a variety of physical, mechanical, and electrical measurements for Nafion and Nafion/titania composite membranes. Some are standard measurements, such as weight gain, dimensional changes, and tensile testing. Other measurements are less common, including long-term creep, swelling pressure, and proton conductivity under load. Several of these new measurement techniques permit us to follow the dynamic changes of polymer ionomers. These measurements give greater appreciation of the complex property changes of the polymer membranes in the environment of a fuel cell.

EXPERIMENTAL

Membrane Preparation

Extruded Nafion 115 films (DuPont) were used as the base material against which other membrane formulations were compared. Recast Nafion membranes were prepared from a 15 wt % Nafion solution (Liquion 1100, Ion Power) mixed with isopropyl alcohol (IPA). The solution was cast onto a flat, glass surface, and the solvent was removed at ~70 °C. After the solvent was removed, the membranes were annealed at ~165 °C for 1 h. To obtain uniform, high-purity films, the membranes were cleaned with a standard treatment procedure: (1) boiling in 3% hydrogen peroxide for 1 h to oxidize organic impurities, (2) rinsing with boiling water for 1 h, (3) boiling in 0.5 M sulfuric acid for 1 h to remove ionic impurities, and (4) rinsing again in boiling water to remove any excess acid.

Nafion/TiO_2 composite membranes were prepared by the recasting of a 15 wt % Nafion solution

(Ion Power) mixed with a solvent [IPA, ethanol (EtOH), or dimethyl sulfoxide (DMSO)] and TiO_2 particles. A variety of different sources and preparations of TiO_2 particles have been examined. In this article, we focus on 21-nm TiO_2 particles (anatase) from Degussa-Huls. To prepare a composite membrane, a colloidal suspension of the TiO_2 particles and one of the solvents was created by the sonication of the particles in the solvent for over an hour. A Nafion solution was added to the suspension, and it was further sonicated. This suspension was cast onto a flat, glass surface, and the solvent was removed by evaporation at ~80 °C in a vacuum oven (for DMSO) or at ~70 °C without a vacuum (for IPA and EtOH). Once the solvents were completely removed, the membranes were annealed via heating to a temperature of ~165 °C for 1 h. The membranes were then cleaned and converted to the H^+ form according to the procedure detailed previously.

Fuel Cell Tests

MEA Preparation

Commercial gas-diffusion electrodes (20% Pt on carbon, 0.4 mg of Pt/cm^2; purchased from E-TEK) were brushed with 5 wt % solubilized Nafion (Aldrich) to impregnate the active layer (0.6 mg/cm^2) and then dried at 80 °C for 1 h. The geometrical area of the electrodes was 5 cm^2. A membrane was sandwiched between two electrodes and gas-sealing gaskets, and then the MEA was pressed for 2 min at 135 °C at 2 MPa with a Carver hot press.

Single-Cell Test Fixture and Performance Evaluation

The MEAs, coupled with gas-sealing gaskets, were placed in a Globe Tech, Inc., single-cell test fixture described elsewhere.[36] The H_2 and O_2 (BOC) gases were fed to the single cell at 100 sccm. The gases were bubbled through water in temperature-controlled stainless steel bottles to fully humidify the feeds before entry to the fuel cell. The baseline test was performed at a total pressure of 1 bar, cell temperature of 80 °C, and anode and cathode humidifier bottles at 90 °C. The fuel cell performance was characterized by current–voltage measurements (polarization curves). These were recorded at 80 °C and atmospheric pressure.

We obtained current–voltage, iv, measurements by connecting the fuel cell to a load resistance (an electronic Amrel load) and sweeping the voltage from 1 to 0.2 V at 10 mV/s, recording the voltage and current. Because the entire current–potential curve for a given temperature/humidification condition was obtained in ~2 min, it was assumed that the membranes had a constant water content throughout the measurement. The fuel cell was preconditioned by operation at 0.5 V for 2–3 h before the iv measurement.

Physical/Chemical Characterization

The ion-exchange capacity (IEC) was determined by an exchange of acidic protons with another cation in solution.[37,38] The membranes were dried and weighed and then placed in a 1 M NaCl solution at 80 °C overnight to exchange Na^+ ions with H^+. The large excess of Na^+ ions ensured virtually complete exchange. The membranes were removed from the solution, and the solution was titrated to the phenolphthalein end point with a 0.1 M NaOH solution to determine the quantity of exchanged H^+ ions. The IEC and equivalent weight (g of polymer/mol of H^+) were calculated with the dry weight of the polymer and the quantity of exchanged protons.

The membranes (~3 cm × 3 cm × 127 μm) were vacuum-dried at ~80 °C for 3 h and then weighed, and the length was measured. The water uptake was measured for membranes placed both in and above liquid water for 24 h at 25 °C and for membranes placed in boiling water for ~1 h. The membranes were removed from the water, blotted to remove droplets, and then weighed and measured. The linear expansion factor ($L\%$) and H_2O sorption ($W\%$) were obtained with eqs 1 and 2:

$$L\% = \frac{L_1 - L_0}{L_0} \times 100 \quad (1)$$

$$W\% = \frac{W_1 - W_0}{W_0} \times 100 \quad (2)$$

where L_0 and L_1 are the lengths of the membranes before and after water sorption, respectively, and W_0 and W_1 are the masses of the membranes before and after water sorption, respectively.

Resistivity measurements were carried out with a membrane sheet 0.5 cm wide and 3 cm long. The membrane was placed between two polycarbonate plates. The top plate had two flush-fit stainless steel electrodes 2.54 cm apart. The alternating-current (ac) impedance across the membrane was obtained at several frequencies from 0.1 Hz to 100 kHz. We found no change in the impedance from 10 Hz to 20 kHz. To record dynamic

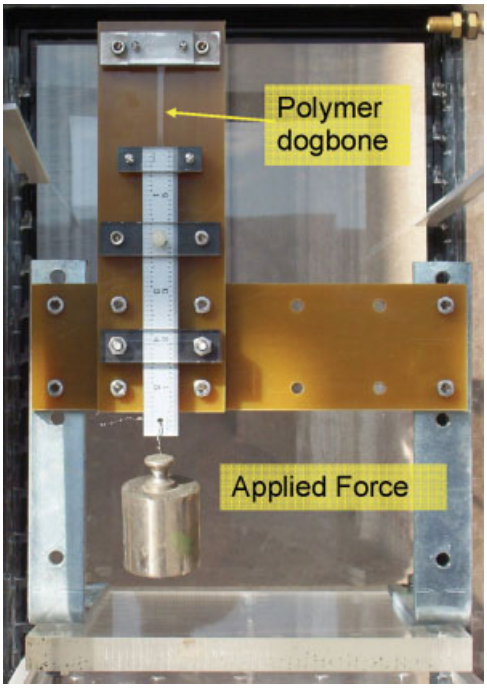

Figure 1. Apparatus for creep measurements of polymer membranes. The entire apparatus fit inside an acrylic box and was placed in an oven.

changes in resistance, the membrane was made one leg of a voltage divider. A driving voltage of 100 Hz was applied across the membrane in series with a fixed 1-kΩ resistor. A pair of ac voltmeters measured the voltage drops across the membrane and the membrane in series with the fixed resistor. The dynamics of the change in the resistance of the membrane could be determined with a response time of $\sim$0.5 s.

Mechanical Testing

Tensile Tests

The membranes were cut into ASTM standard dog-bone samples with a gauge length of 2.2 cm and a width of 0.5 cm. The samples were tested in an Instron with a constant strain rate of 5 cm/min. The testing chamber was heated to temperatures in the range of 20–120 °C. The water content was varied by the preconditioning of the samples in controlled-humidity environments (above saturated salt solutions). At room temperature, the water evaporation was sufficiently slow that the water content per sulfonic acid group did not change by more than 2 during the test. To test samples at higher temperatures without the loss of water, the dog bones were positioned inside a Ziploc polyethylene bag, and the samples and Ziploc bag were clamped in the grips of the Instron. The Ziploc bag was kept slack so it added a negligible contribution to the stress when each sample was strained. The membrane water content during the test was determined by the weighing of the sample before and after the test. The dry weight of the sample was determined after drying at 170 °C for 24 h. All tested samples contained Nafion EW 1100, so the water content per sulfonic acid residue (λ) was calculated with eq 3:

$$\lambda\left(\frac{\text{mol } H_2O}{\text{mol } SO_3^-}\right) = \frac{(M_{Test} - M_{Dry}) \cdot \frac{1 \text{ mole } H_2O}{18.015 \text{ g } H_2O}}{\frac{M_{Dry} \cdot (1 - Wt\%TiO_2)}{EW^{g \text{ Membrane}}/\text{mol } SO_3^-}} \quad (3)$$

where M_{Test} is the mass (g) of the sample during the test and M_{Dry} is the mass after drying at 170 °C for 24 h.

The Young's modulus and plastic modulus were determined for each sample and plotted as a function of the temperature and λ value. (The plastic modulus, as we apply the term, refers to the change in the stress with strain beyond the yield point, which is a measure of the strain hardening of the material.) The tested membranes included extruded Nafion, Nafion recast with 0, 0.5, 1, 3, 6, or 20 wt % TiO_2 and purchased from Degussa-Huls, Nafion recast with 3% TiO_2 and purchased from Alfa-Aesar, Nafion recast with 3% rutile needles, and Nafion recast with 3% Degussa-Huls TiO_2 with the solvents IPA, DMSO, and EtOH. Although different solvents were tested, we saw no distinction between the membranes cast from these three solvents.

Creep Testing

The effect of a constant stress on the different membrane materials was evaluated by the measurement of their creep. The membranes were cut into ASTM standard dog-bone samples with a gauge length and width of 2.2 cm and 0.5 cm, respectively. Polymer dog bones of 115 membranes were cut and clamped in the apparatus shown in Figure 1. The entire apparatus was placed inside an acrylic box with beakers of saturated salt water baths to control the water activity, and the acrylic box was placed in an oven. A weight was hung from the bottom of the dog bone, and the polymer strain was recorded as a function of time.

Dynamic Water Uptake and Conductivity

Water sorption by Nafion and Nafion/titania composite membranes was measured at several differ-

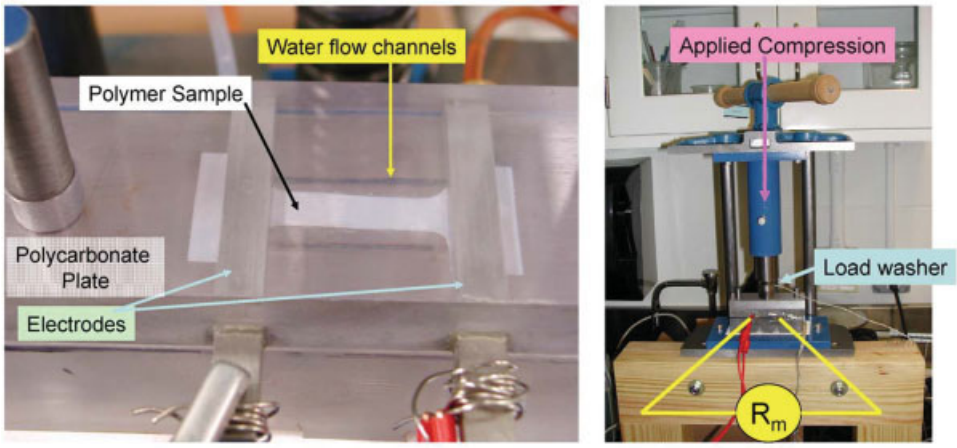

Figure 2. Resistance measurement cell for membranes in a confined environment. The water flow goes through the channels on the bottom plate (shown in the left rear). The membrane sits between the two plates and absorbs water. The polycarbonate plates sit beneath the load washer. The membrane resistance (R_m) is determined across the stainless steel electrode in the upper plate. The cell is compressed: a screw drive compresses a spring in the blue cylinder above the load washer (right).

ent temperatures from 25 to 75 °C. The membranes were dried in an oven at 130 °C for 1 h and used immediately. Dry samples were suspended on a Teflon thread from a bottom weighing balance. After the determination of the dry weight, the sample was positioned inside a three-necked flask half-filled with water. The flask temperature was controlled by a heating tape wrapped around the flask. A thermocouple was positioned in one neck of the flask to monitor the temperature. The temperature was constant to ±1.5 °C over the course of the experiment. The mass increase was recorded as a function of time for ~4000–5000 s. A combination temperature/relative humidity (RH) sensor placed where the membrane samples normally hanged verified that the test conditions were 95–100% RH and the same temperature reported by the thermocouple.

Membrane Proton Conductivity

A polymer membrane in a fuel cell is in a constrained environment under compression. To examine the effect of compression on the proton conductivity, the apparatus shown in Figure 2 was built. Polymer dog bones were placed in the compression cell shown in Figure 2(A). The bottom plate had two 1 mm × 1 mm × 15 mm channels with water running through them. The top plate had two stainless steel cross bars machined flush with the polycarbonate, which ran perpendicularly to the water flow channel in the bottom plate. The central section of the dog bone was positioned between the two flow channels. The flow channels were filled with water to maintain the water activity in the membrane at unity (the membranes did not lose any water by evaporation during the compression measurements).

Three types of measurements were performed: (1) the membrane resistance was measured as a function of the compressive stress on the membrane, (2) the membrane resistance was measured as a function of time at a constant stress, and (3) the membrane resistance was measured as the constrained membrane absorbed water. In the first experiment, the stress was increased from 0 to 7.25 MPa in incremental steps every minute, and then the pressure was reduced back to 0 in the reverse sequence. The entire cycle took 20 min. The second experiment consisted of permitting the membrane to equilibrate for ~2 h at a fixed stress and then changing the stress and following the resistance as a function of time.

For the third set of experiments, rectangular samples (5 cm × 2.5 cm) were prepared with two 2.5 mm × 20 mm slots cut out of the membrane in the area of the water flow channels.

A load was imposed on the top plate [Fig. 2(B)]. The force of the load was measured via a load washer. A heavy-duty die spring kept the applied load fixed while allowing the membrane to expand or contract with the water uptake. The resistance of the membrane was measured by the application of an ac voltage across the membrane in series with a 1-kΩ resistor. The ac voltages across the

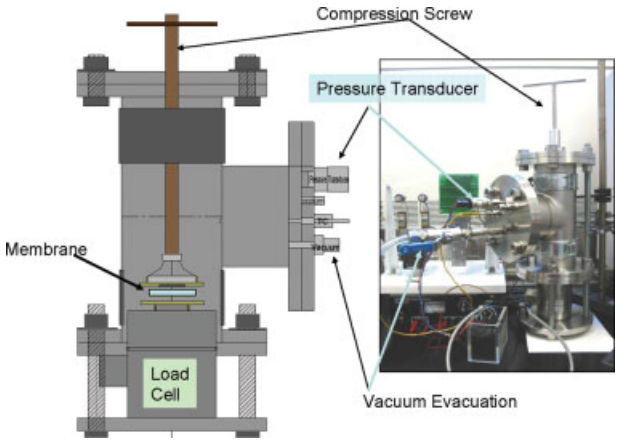

Figure 3. Swelling pressure measurement device. The entire cell was placed inside an insulated box (not shown) to maintain a uniform temperature.

1-kΩ resistor and the membrane and resistor in series were measured to determine the membrane resistance. In principle, the capacitance of the circuit could also be measured, but we found that the capacitance was negligible for the nonporous, stainless steel electrodes, so there was negligible phase lag for frequencies greater than 1 Hz.

The dynamics of water sorption were measured by the resistance of a membrane as it absorbed water. In a typical transient experiment, the water channels were dried thoroughly, and a dry membrane was positioned in the cell and clamped with a specified force. A peristaltic pump was used to flow water through the flow channels. The water flow rate was typically $\sim$10 mL/min, but the results were not dependent on the water flow as long as the flow channels stayed filled with liquid. The resistance of the membrane was measured as a function of time.

Swelling Pressure

The swelling pressure was measured in the environmental compression cell shown in Figure 3. Samples (1.4-cm discs) were cut from sheets of Nafion 115 and Nafion/TiO_2 115 composite membranes that were equilibrated at the ambient temperature and RH. After drying at 130 °C for 1 h, the samples were $\sim$1.2 cm in diameter and were positioned between porous, stainless steel frits and compressed by a threaded screw. This apparatus had a fixed strain, as opposed to the fixed stress system used in the conductivity measurements. After vacuum evacuation of the chamber, the water vapor pressure was increased by the injection of known aliquots of water. The polymer absorbed water and swelled. A load cell measured the force generated by the membrane as it swelled with water sorption. We simultaneously measured the temperature, RH, total gas pressure, and force generated by the membrane.

RESULTS

Fuel Cell Response and Water Sorption

Figure 4 shows the iv curves for fuel cells containing a Nafion 115 extruded membrane and a Nafion 115/3 wt % TiO_2 membrane. Both membranes had a nominal thickness of $\sim$127 μm. The voltages obtained at the same current density were greater with the composite membrane than those obtained with Nafion. The *in situ* resistivity of the membrane was estimated from the slope of the iv curve in the ohmic region. The composite membrane had a resistivity of 20 $\pm$ 2 Ω cm, whereas the Nafion membrane had an estimated resistivity of 30 $\pm$ 4 Ω cm. Fuel cell tests for temperatures from 60 to 120 °C with fully humidified feeds did not show any measurable difference in the membrane resistivity for either of the membranes.

Physical/Chemical Characterization

Table 1 compares the density, dimensional change with water sorption, IEC, and proton conductivity for the Nafion and Nafion/TiO_2 composite membranes. The fractional mass gain for both sets of membranes was the same to within 3%; contrary to many reports in the literature,[11,39,40] we found no difference in water sorption between liquid and vapor after 24 h in a sealed container. Membranes placed in water at 100 °C for 1 h absorbed almost twice the amount of water as membranes placed in water at 25 °C for 24 h.

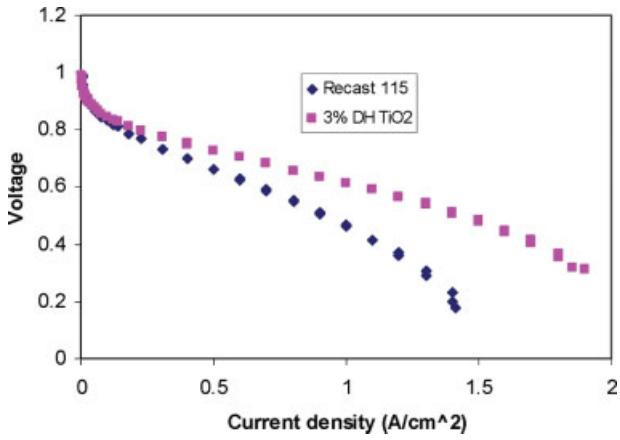

Figure 4. Current–voltage sweep of fuel cells at 80 °C with fully humidified feeds for Nafion 115 and Nafion 115/3 wt % 21-nm TiO_2 particle composite membranes.

Table 1. Physical Characteristics of Nafion and Nafion/Titania Composite Membranes

Membrane	Dry Density (g/cm^3)	Wet Density (g/cm^3)		IEC (μequiv/g)	Water Swelling ($\Delta L/L$)		Resistivity at 23 °C and 100% RH (Ω cm)
		23 °C	100 °C		23 °C	100 °C	
Nafion 115 (extruded)	1.92 ± 0.08	1.65 ± 0.08	1.42 ± 0.08	950 ± 25	0.10 ± 0.01	0.20 ± 0.01	12.4 ± 0.5
Nafion 115 (recast)	1.96 ± 0.10	1.68 ± 0.08	1.44 ± 0.08	960 ± 25	0.12 ± 0.01	0.24 ± 0.01	10.6 ± 0.5
Nafion/titania 115 (3 wt %)	1.94 ± 0.11	1.68 ± 0.08	1.50 ± 0.08	970 ± 25	0.12 ± 0.01	0.23 ± 0.01	9.3 ± 0.5

After being weighed, the membranes that had been removed from boiling water were placed in beakers of water at room temperature for 24 h and then reweighed. The mass of the membranes was the same as that determined immediately after their removal from water at 100 °C. This simple experiment demonstrates that water sorption by Nafion-type membranes can be controlled by kinetics; water sorption is not thermodynamically equilibrated within 24 h at 25 °C, and substantial hysteresis can exist, depending on the history of the membrane.

There was no measurable difference in the swelling behavior or IEC of Nafion and Nafion/TiO_2 membranes. The resistivity of the membranes measured *ex situ* is about a factor of 2 less than the resistivity inferred from the ohmic region of the iv curve in the fuel cell. Part of the difference in the resistivity is due to using the nominal thickness of the membrane (127 μm) to determine the resistivity in the fuel cell. The membrane thickness increases from water sorption. The transverse resistivity (across the membrane as it would be measured in the fuel cell) scales with the membrane thickness. The longitudinal resistivity (measured in the *ex situ* device) scales inversely with the thickness. If the membrane thickness is swollen by 25%, the *in situ* fuel cell resistivity is increased by 25%, whereas the *ex situ* resistivity is reduced by 25%. Making these corrections brings the values in Table 1 into close agreement with the resistivity determined from the slope of the iv curve shown in Figure 4.

Mechanical Properties

Tensile Tests

Water sorption is accompanied by membrane swelling, which depends on the mechanical properties of the polymer or composite. We have looked at several different mechanical property measurements of the membrane materials. The most common polymer tests are tensile tests. A typical tensile test for extruded Nafion and a Nafion/titania composite membrane is shown in Figure 5. A variety of values can be extracted from the tensile testing; we focus on two properties, the elastic modulus (the slope of the stress–strain curve at small strains) and the plastic modulus (the slope of the stress–strain curve beyond the yield point). A true plastic would show no increase in stress with increasing strain above the yield point. Nafion showed increasing stress as it was strained past the yield point. A positive slope of the stress–strain curve past the yield point is indicative of strain hardening.[41,42]

Figures 6 and 7 summarize our stress–strain measurements for Nafion and Nafion/titania composite membranes. As expected, Figure 6 shows that the elastic modulus decreases with increasing temperature. At room temperature, the elastic

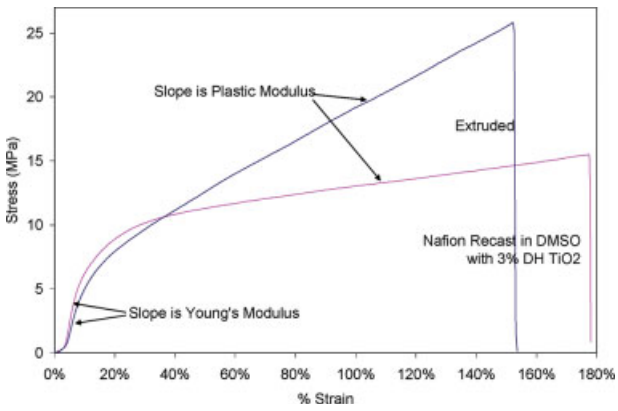

Figure 5. Stress–strain response of extruded Nafion and Nafion/titania composite membranes. The strain rate was 5 cm/min. The data were obtained at room temperature (22–25 °C). The water content for each membrane was $\lambda \sim 10.9$ H_2O/SO_3.

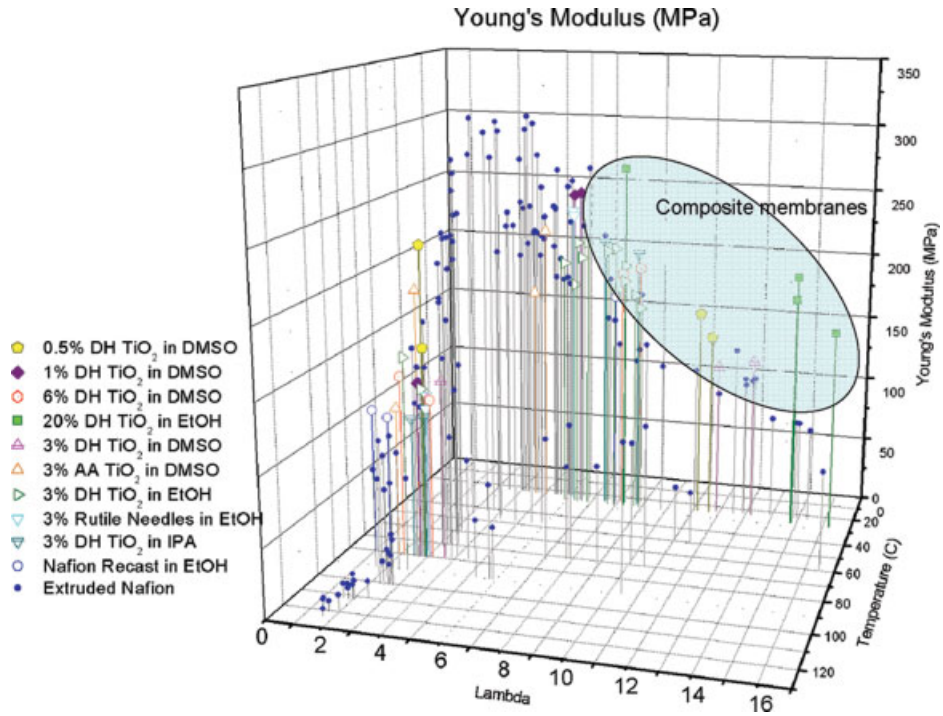

Figure 6. Elastic modulus of Nafion and Nafion/titania composite membranes. Each point represents a different sample. A variety of Nafion/titania composite samples have been included on this graph to illustrate the magnitude of the effect with increased loading.

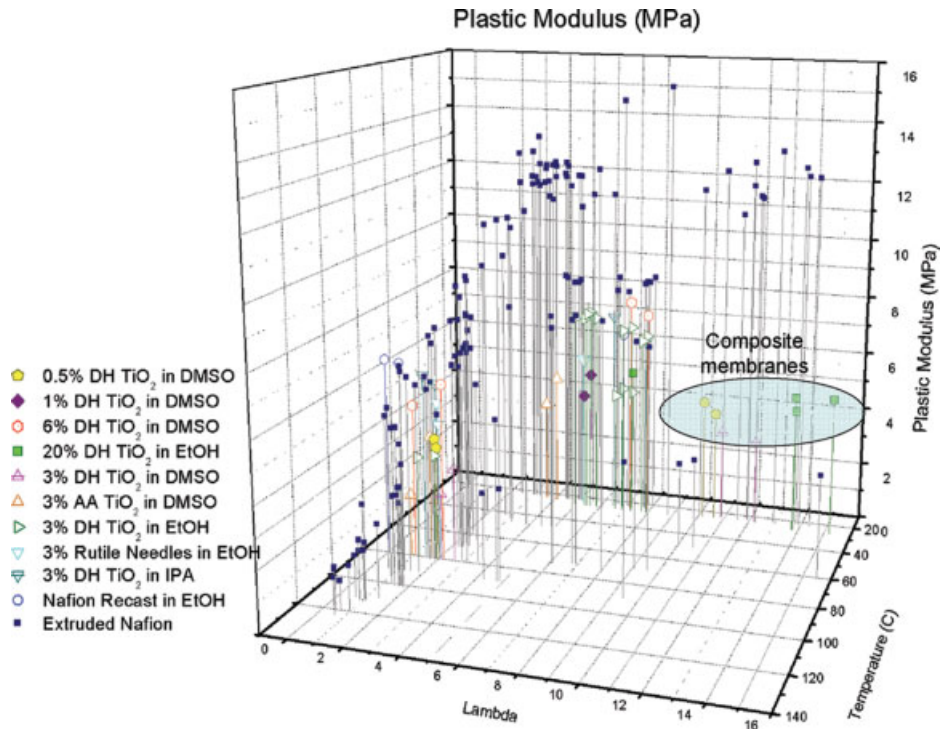

Figure 7. Plastic modulus of Nafion and Nafion/titania composite membranes. A variety of Nafion/titania composite samples have been included on this graph to illustrate the magnitude of the effect with increased loading.

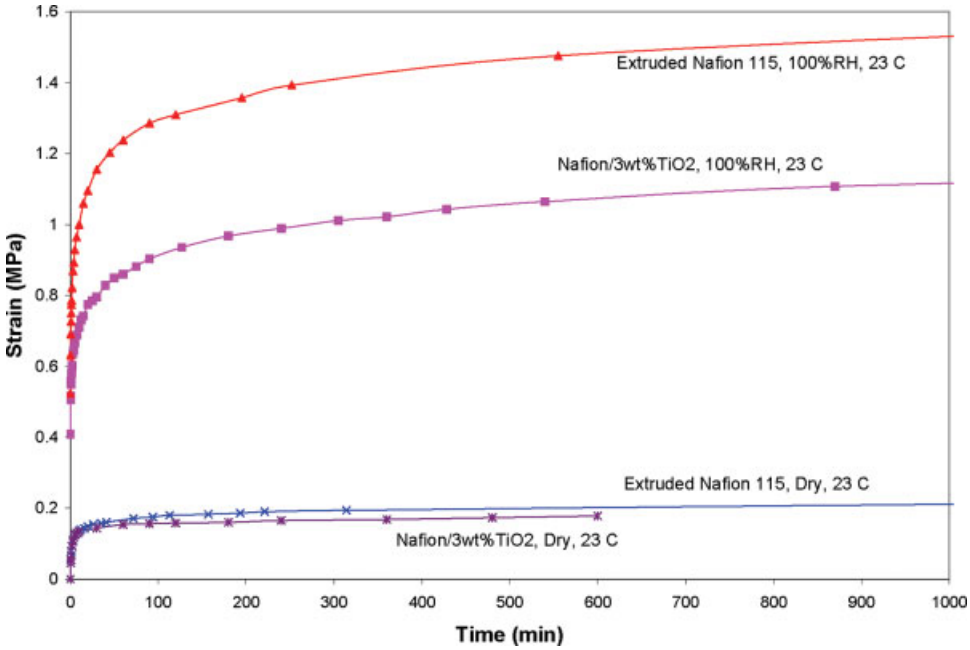

Figure 8. Creep data for Nafion 115 and Nafion/3 wt % titania 115 at 23 °C for both 0% RH (dry) and 100% RH with an applied engineering stress of 7.5 MPa.

modulus is ~300 MPa, and it decreases to ~100 MPa at 80 °C (the normal operating temperature for PEM fuel cells). The elastic modulus drops precipitously to less than 10 MPa above 100 °C. The large decrease in the elastic modulus coincides with T_g, which has been reported to be 110 °C.[17,20,43] Absorbed water also reduces the elastic modulus; the elastic modulus at 25 °C decreases from 300 to 50 MPa as the water content in the membrane increases.

The plastic modulus of Nafion (Fig. 7) shows a weaker dependence on the temperature and water content than the elastic modulus. The plastic modulus is almost independent of the temperature below T_g ($T_g \sim 110$ °C) with a value of ~8–10 MPa, and it decreases to ~2 MPa above T_g. At room temperature, the water content in the membrane has little measurable effect on the plastic modulus.

We have found two key results when comparing the properties of Nafion and Nafion/titania composites: (1) water sorption reduces the elastic modulus of Nafion more than that of Nafion/titania composites and (2) water sorption reduces the plastic modulus of Nafion/titania composites more than that of Nafion. The temperature affects the mechanical properties of Nafion and Nafion/titania composite membranes comparably. Composite materials generally have higher elastic moduli, but at the low loading of 3 wt % (~1.5 vol %), we did not see much effect in the dry materials. The effects of adding the metal oxide particles were manifested at higher membrane water contents.

Creep Tests

During the normal operation of a fuel cell, electrodes are pressed against the polymer electrolyte membrane, and this puts the polymer under compressive stress. The effect of constant tensile stress on two different membrane materials was evaluated by the measurement of their creep. Figure 8 compares the creep responses of an extruded Nafion 115 membrane and a Nafion/3 wt % TiO_2 115 membrane. Nafion 115 crept nearly 40% more than the composite membrane over a period of 3000 min (>2 days) when subjected to the same stress.

Both the polymer and composites stretched rapidly over the first several minutes (the short-time response is blown up in the inset in Fig. 8). After ~1–10 min, the polymer membrane strains much more slowly. Polymer creep data can be fit to various functional forms, including stretched exponentials derived from spring-dashpot models. The data shown in Figure 8 are linear when plotted as the strain versus log(time) for times from 10 s to

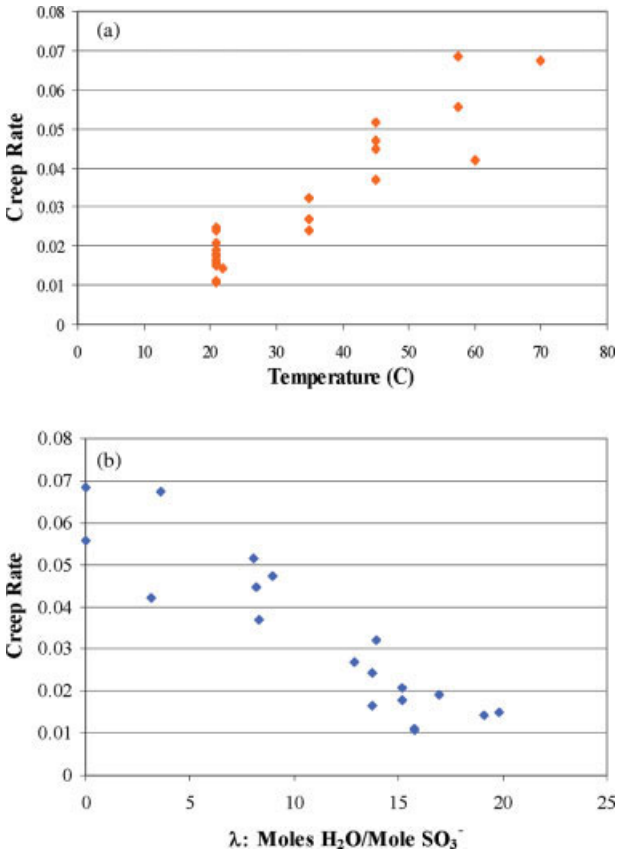

Figure 9. Long time creep rate (defined by eq 4) of Nafion 115 (A) as a function of temperature at a fixed water content of $\lambda \sim 8 \pm 2$ H_2O/SO_3^- and (B) as a function of the water content at 21–25 °C.

greater than 10^4 s. For fuel cell performance, we are principally interested in the long-time creep, and we have defined the creep rate (eq 4) as the slope of the strain–log(time) response at times greater than 100 min, normalized by the applied stress:[44,45]

$$\text{Creep Rate} = \frac{\mathrm{d}\left[\frac{\text{strain}}{\text{stress}}\right]}{\mathrm{d}[\log(\text{time})]} \tag{4}$$

Figure 9 shows the creep rate of extruded Nafion 115 membranes as a function of the temperature and water content. We determined the water content by weighing the membranes immediately after the creep measurements. At a fixed stress, the creep rate increased with increasing temperature and decreased with increasing water content. The reduced creep rate with an increased water content, shown in Figure 9, would appear to be at odds with Figure 8, in which a higher water content leads to greater total creep. This apparent discrepancy is because the creep rate refers to long times. Samples with higher water contents crept faster initially, but the rate of creep slowed more at longer times. The dry samples crept less initially but continued to creep more at longer times.

Dynamic Water Uptake

Figure 10 shows typical results for the water uptake from saturated vapor for unconstrained samples of extruded and recast Nafion/titania composite membranes at various temperatures. The same three materials reported in Table 1 were used for the data shown in Figure 10. The results show that water was absorbed faster at higher temperatures and that recast Nafion membranes, with or without titania, absorbed water faster than extruded Nafion. The results for equilibrated water sorption given in Table 1 show small differences in the water sorption between the three different materials. It appears that the kinetics of water sorption is sensitive to the method of preparation. This is not surprising considering because others have reported different microstructural morphologies (based on small-angle X-ray scattering experiments) between extruded Nafion and solution-cast Nafion.[46] The extrusion process results in orientation of the material's microstructure, and this leads to differences in the physical properties (viz., electrical conductance and swelling). Because solvent transport is linked to both the degree of swelling and morphology, the kinetics of water absorption should differ for recast and extruded Nafion.

The water diffusivity (D) was estimated by the fitting of the data at a low water uptake to eq 5:[12]

$$D = \left(\frac{M}{M_\infty}\right)^2 \frac{\pi \ell^2}{16t} \tag{5}$$

where M/M_∞ is the mass uptake at time t with respect to the mass uptake after 24 h and ℓ is the initial membrane thickness. A value of $\sim 1 \times 10^{-8}$ cm^2/s was obtained for the diffusivity. However, the diffusivities for the recast membranes were lower than those for extruded Nafion. This result was disturbing because the recast membranes sorbed water faster than extruded Nafion. The problem with this analysis for diffusivities is that it fails to account for the energy changes and dimensional changes that accompany water sorption. Values of diffusivities are not reported

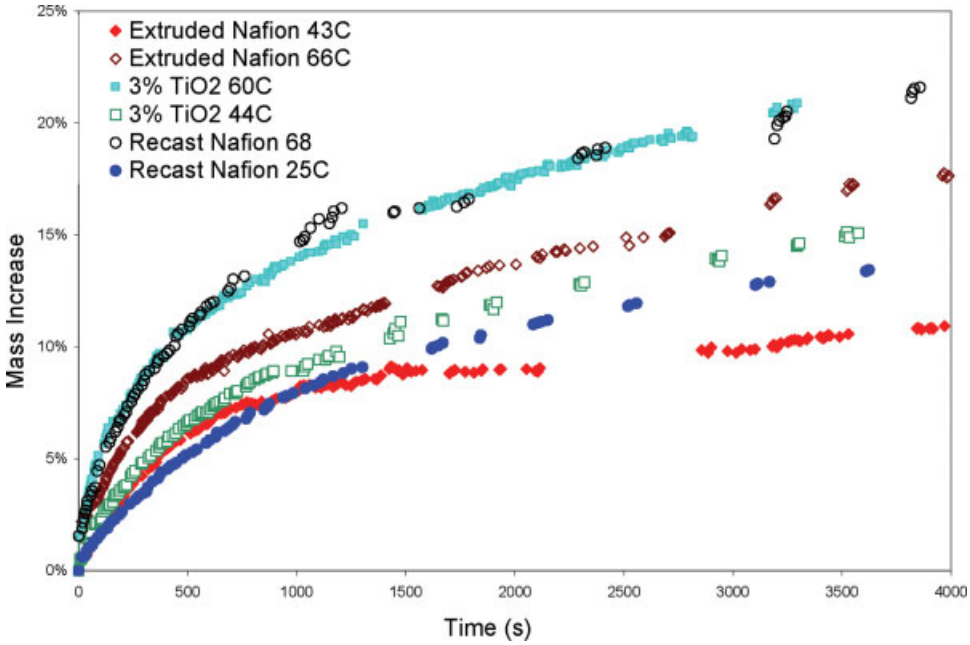

Figure 10. Mass gain of Nafion and Nafion/titania composite membranes from saturated water vapor at different temperatures.

because the simple analysis misses key physics associated with the water sorption process. The drying temperature before absorption, 130 °C for 1 h, is higher than those used by other researchers, who dried Nafion below its T_g of 110 °C to avoid disturbing its microstructure.[39,47] However, drying at 130 °C more closely matches the conditions at which an MEA is hot-pressed, and this is relevant to the changes encountered during water absorption in a fuel cell. The effect of the thermal history on membrane water absorption is an important question, but a complete study is beyond the scope of this article.

The dynamics of water absorption were also seen in the changing membrane resistance as it absorbed water inside the device depicted in Figure 2. A typical result is shown in Figure 11 for a membrane under a compressive load of 40 kPa at 21 °C. Figure 11 shows that water was rapidly absorbed into the membrane, reducing the resistivity by over an order of magnitude in the first 100 s. The rate of change of the resistivity slowed dramatically after the initial decrease. The membrane resistivity kept decreasing for ~100,000 s. The membrane resistivity decreased from 60 to 15 Ω cm between 1000 s and 5000 s and to less than 13 Ω cm after 20,000 s. It reached its equilibrated resistance of 12.6 Ω cm after 40,000 s. The resistivity decreased slightly faster for a Nafion/titania (3 wt %) 115 membrane than extruded Nafion 115 at room temperature; this is consistent with the water uptake measured by the change in mass. Preliminary experiments have shown that the resistivity change is slowed by an increasing applied load, but we do not yet have sufficient data to quantify these phenomena.

Membrane Proton Conductivity

A polymer membrane in a fuel cell is in a constrained environment under compression. Figure 12 shows the resistivity as a function of the applied stress on the membrane for both extruded Nafion 115 and Nafion/3 wt % TiO_2 115 membranes. The resistivity was based on the dry membrane thickness. The stress was increased from 0 to 7.25 MPa in incremental steps every minute. After 1 min at each applied stress, the resistivity change was slow (<2%/min), but we did not wait for full equilibration. The membrane resistivity had increased by ~15% at the maximum applied stress of 7.25 MPa. After the maximum was reached, the stress was reduced with the reverse sequence. There was a substantial hysteresis in the resistance at the same stress level on the return path. We did find that the resistivity at ~0 stress was recovered but only after ~1000 s. This hysteresis of the resistance with stress was reproducible.

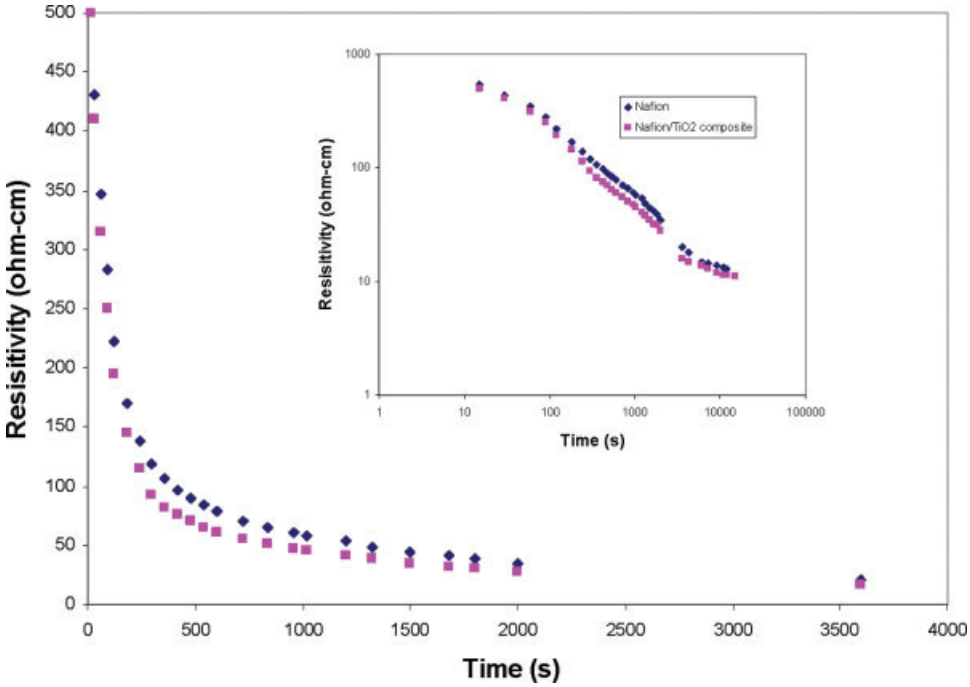

Figure 11. Resistance change of a Nafion 115 extruded membrane and a Nafion/3 wt % titania 115 membrane due to water uptake as a function of time. The inset graph shows the data plotted on a log–log scale.

To better understand the resistivity hysteresis with changing stress, the resistivity was recorded as a function of time after a step change in the membrane stress. Figure 13 shows the dynamic response of the membrane resistance. The results show that the resistivity does not equilibrate to the same value after 1000 s; there is a substantial difference in the membrane resistivity depending

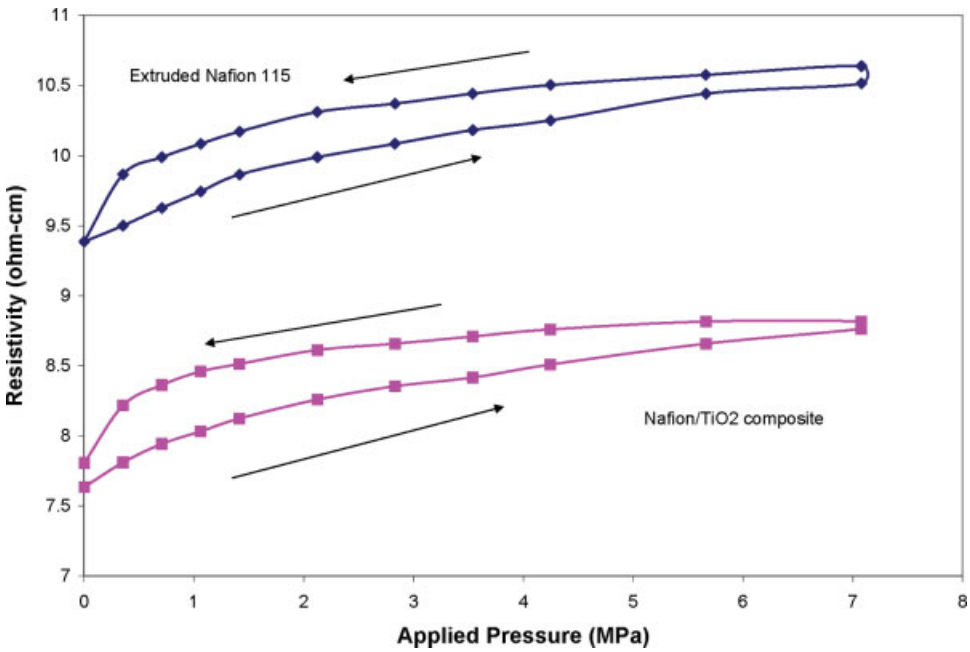

Figure 12. Polymer resistivity as a function of the applied stress on the membrane. The membranes were equilibrated in water at room temperature, and the water activity in the compression cell was maintained at unity.

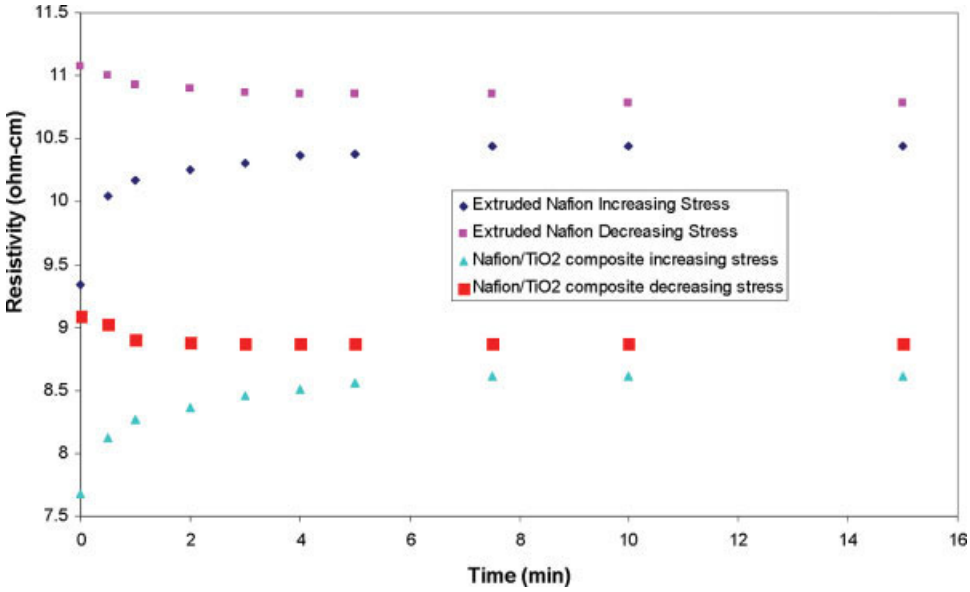

Figure 13. Resistivity change during the stress relaxation of Nafion and Nafion/TiO_2 composite membranes.

on the direction of approach to the applied stress. The stress relaxation hysteresis shown in Figure 13 persisted for more than 200 min with both membranes. Both membranes relaxed back to their zero stress resistivity in approximately 10 min if the applied stress was completely removed.

Dynamics of Membrane Swelling

Membrane swelling associated with water sorption requires the membrane to develop sufficient internal pressure to overcome the applied stress compressing the membrane. The energy of water sorption per unit of volume gives rise to a swelling pressure of the membrane, as measured by the device depicted in Figure 3. Typical data are shown in Figure 14(A,B). Both extruded Nafion 115 and Nafion/3 wt % TiO_2 115 membranes generated a swelling pressure of 0.55 ± 0.03 MPa for water sorption at 60–90 °C. The swelling pressure changed by less than 10% between 30 and 90 °C. Figure 14(B) is a blowup of the force generated when water is injected and shows that the water sorption and swelling pressure build up quickly within ~100 s. After the initial increase in force, there is a slow decrease in the force with a much longer response time, ~10,000 s. The slow relaxation to the swelling pressure occurs with a time response similar to that of membrane creep. From limited data for composite membranes, the swelling pressure of the Nafion/3 wt %TiO_2 composite membranes is the same as that of Nafion within the experimental error.

DISCUSSION

The studies reported here were initiated to elucidate how polymer electrolytes in constrained environments respond to applied stresses. The membrane in a PEM fuel cell is constrained between the porous electrodes; the compression sealing of the fuel cell assembly puts the membranes under stress. As the polymer electrolyte absorbs and desorbs water, it swells and shrinks, altering the stress levels and proton conductivity. There is precious little data available concerning the mechanical properties of polymer electrolytes as functions of both the temperature and water activity, and there is virtually no data for the properties of these materials in confined environments. The data presented here are by no means complete, but they begin to elucidate how water and temperature affect the mechanical and electrical properties of polymer electrolyte membranes, which may impact fuel cell performance.

The addition of TiO_2 particles to a Nafion membrane improves the fuel cell performance. These improvements have been documented by us and others.[36] There have been several different explanations for this improvement; most of the theories have focused on greater water sorption in the composite membranes, particularly under reduced-humidity conditions.[5,31,48] The fuel cell data shown in Figure 4 were obtained under fully humidified conditions and show that the composite membrane had lower resistivity even at full hu-

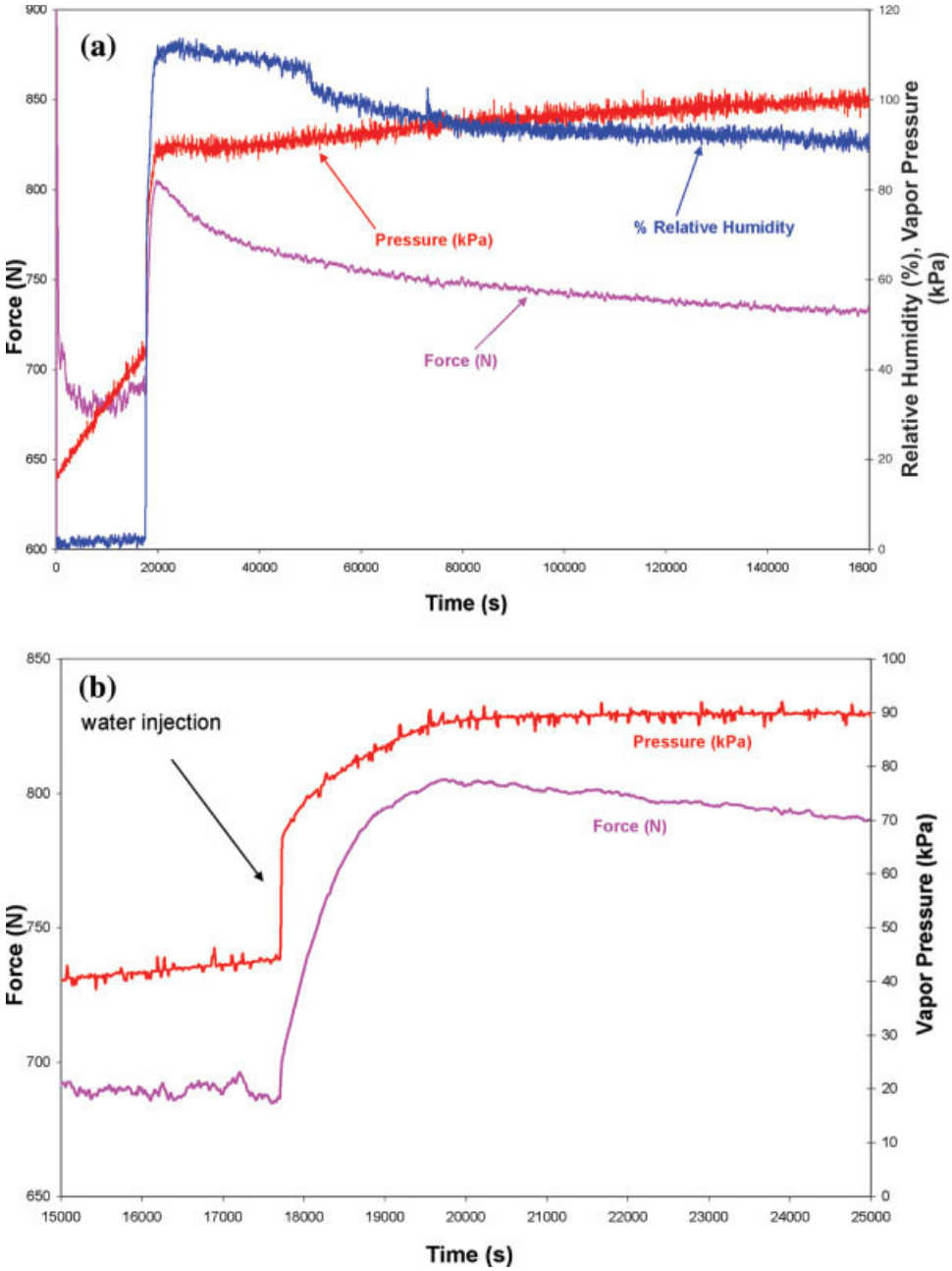

Figure 14. (A) Swelling measurement of Nafion 115 at 90 °C. Water was injected at 17,250 s, increasing the RH from 0 to 100%. The gas pressure inside the chamber rose slowly over time because of a small leak in the septum. (B) Swelling of Nafion 115 after water injection. This is a blowup of part A around the time of the water injection. It shows the timescale for the water uptake and the swelling pressure buildup to be ~500–1000 s.

midification. Also, the measurements of equilibrated water sorption did not show any significant increase in the water content due to the presence of the TiO_2 particles. Dynamic measurements of water sorption showed that the recast membranes with and without particles had higher water sorption rates than extruded Nafion. The high sorption rates correlated with reduced resistivity in the recast Nafion and Nafion/TiO_2 membranes. These results suggest that recasting modifies the microstructure of Nafion membranes, facilitating water diffusion and proton mobility.

The membranes become less stiff with increasing temperature and increasing water content. Both the elastic and plastic moduli decrease gradually with increasing temperature up to ~100 °C; above the T_g of ~110 °C, the elastic modulus decreases by over an order of magnitude. The plastic modulus also decreases with increasing temperature and drops at T_g. Water plasticizes Nafion. From Figure 6, it is evident that at 25 °C, the elastic modulus decreases by almost a factor of 6 from a dry membrane to a water-saturated membrane. This decrease in the elastic modulus is comparable to that observed when the temperature of a dry Nafion membrane is increased from 25 to 80 °C. Water sorption has a much smaller effect on the plastic modulus, as shown in Figure 7. The mechanism for strain hardening does not show a strong dependence on the water content in the polymer.

The plasticizing effect of water and temperature on the elastic modulus of the membranes can explain why water sorption increases with increasing temperature. Water sorption by the sulfonic acid moieties is an exothermic process, and as such, it would be expected that water sorption should be greater at lower temperatures. However, it has been documented by many investigations that water sorption by Nafion increases with increasing temperature.[48–51] The total energy change due to water sorption (E_{sorption}) is the sum of the chemical energy of water solvating the sulfonic acid groups and the mechanical energy of swelling the membrane, as expressed in eq 6. The first term in the integral is the heat of solvation, and the second term is the work of polymer swelling. Both the solvation energy and the elastic modulus of the polymer decrease with increasing water content. We have approximated these with simple linear functions of λ; $\lambda_{\max} \sim 20$ is the maximum solvation of the sulfonic acid groups. For simplicity, the enthalpy of water sorption has been set to decrease linearly from $-\Delta H_0$ at zero water content to zero at the maximum water uptake, and the elastic modulus, E_0, has been scaled to decrease by a fraction α from its dry state to the fully hydrated state. It has also been assumed that the volume of swelling is linear with the molar volume of water ($\bar{V}_w$):

$$\mathrm{E}_{\text{sorption}}(\lambda) = \int_{\lambda_o}^{\lambda} \left(-\Delta H_o \left(\frac{\lambda_{\max} - \lambda}{\lambda_{\max}} \right) + E_o \left(1 - \alpha \frac{\lambda}{\lambda_{\max}} \right) \bar{V}_w \right) d\lambda \quad (6)$$

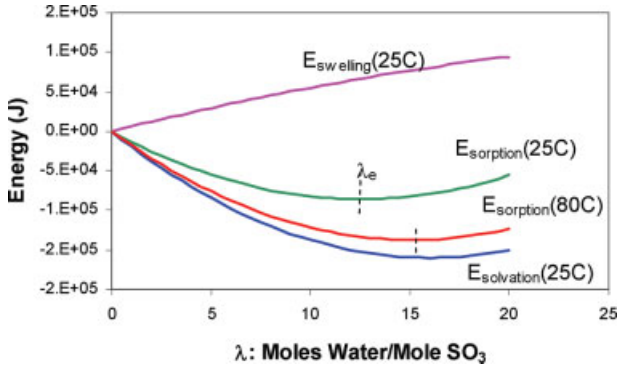

Figure 15. Swelling, solvation, and sorption energy for water into a Nafion membrane [$\Delta H_0 = -20$ kJ/mol, $E_0(25\ ^\circ\text{C}) = 350$ MPa, $\lambda_{\max} = 16$ water/SO_3, $\alpha = 0.4$, $E_0(80\ ^\circ\text{C}) = 100$ MPa].

The equilibrium water content (λ_e) occurs for the minimum in the energy as expressed in eq 7:

$$\lambda_e = \frac{-\Delta H_o + E_o \bar{V}_w}{-\Delta H_o + \alpha E_o \bar{V}_w} \lambda_{\max} \quad (7)$$

Figure 15 shows the total energy of water sorption along with the contributions of the energy of solvation and the energy of swelling based on eq 6. The minimum in the total energy corresponds to the λ_e value predicted by eq 7. As the temperature is increased, the elastic modulus decreases much more than the energy of solvation, and this results in the energy released by solvation being able to further expand the polymer membrane and reduces the total energy of the system. This also shifts the number of water molecules sorbed into the membrane. Figure 15 shows that for typical values of the elastic modulus and solvation enthalpy, the decrease in the elastic modulus from 350 MPa for Nafion at 25 °C to 100 MPa at 80 °C results in an increase in the number of sorbed water molecules from 12 to 16 water/SO_3. The simple model presented here neglects the entropic contributions to the free energy. However, for the large energies associated with water sorption into ionomers, the entropic contribution will be small with respect to the energetic contributions.

It is evident from Figures 6 and 7 that the mechanical properties of Nafion have not been explored in much of the parameter space at elevated temperatures and elevated water activity. A synergistic effect between water plasticizing the material and temperature reducing the mechanical strength is expected. There are a few data points shown on Figures 6 and 7 taken at elevated temperatures with increased water content. Those

data show that the elastic modulus is less than that of a dry membrane at those temperatures or that of a wet membrane at 25 °C. There are not yet sufficient data to identify how T_g changes with the water content.

Adding TiO_2 to make a composite membrane increased the elastic modulus of the membrane at increased water content. This improvement is highlighted in Figure 6. The addition of TiO_2 did not have a significant effect on the temperature dependence of the elastic modulus. A surprising result obtained for the Nafion/titania composite materials was that the plastic modulus decreased. The composite membranes showed less strain hardening than Nafion, especially at high water contents. Figure 7 shows that the plastic modulus of the composite membrane decreased compared with that of Nafion at high water contents and 25 °C. Some Nafion/Zirconia composite membranes that we tested showed a plastic modulus of zero; there was no change in the stress as they were strained.

The results show that modifying membranes with titania causes the mechanical properties of the membranes to be altered more by water than temperature. Because the metal oxide particles are hydrophilic, we believe that they interact strongly with the hydrophilic (sulfonic acid) domains of Nafion. Water sorption alters the interaction between the metal oxide surfaces and the hydrophilic domains of Nafion, and this results in changes in the mechanical properties. We do not yet have sufficient experimental information to quantify the magnitude of the particle/Nafion/water interaction.

The creep experiments showed that the membranes crept over a long time period when placed under moderate stress. It was surprising that Nafion/TiO_2 composite membranes crept much less than Nafion when placed under a constant stress, as shown in Figure 8. It was anticipated that the composite membranes would creep more than Nafion because they had a lower plastic modulus, which indicated less strain hardening; this should have permitted the composite materials to flow more readily. However, most of the creep experiments were performed at stresses less than the yield stress, so there was not a direct connection between the creep and the plastic modulus. Creep does increase with increasing temperature and decreasing water content, as shown in Figure 9(A,B). Creep may play an important role in fuel cell failure; the creep from high stress points may thin out the membrane over time, eventually causing pinholes in the membrane.

The measurements shown in Figures 12 and 13 are some of the first data showing how the compressive forces can alter the resistance of polymer electrolytes. These results also show substantial hysteresis in the membrane resistivity from compression. Membrane resistivity increased by 10–15% for an applied pressure of 7.25 MPa. This increase in resistivity appears to be the result of simple mechanical compression of the membrane and not actually a change in the resistivity. The resistance of the central section of the dog bone is measured lengthwise along the neck of the dog bone. The resistance ($R_{membrane}$) is given by eq 8:

$$R_{membrane} = \rho \frac{L}{Wt} \tag{8}$$

where ρ is the resistivity, t is the membrane thickness, W is the width, and L is the length. When the membrane is compressed, t will decrease by Δt with the applied stress ($P_{applied}$):

$$\Delta t = \frac{P_{applied}}{E} t \tag{9}$$

where E is the elastic modulus. A wet membrane at 25 °C has an elastic modulus of ~50 MPa (see Fig. 6), so an applied stress of 7 MPa will reduce the membrane thickness by 14% and hence increase the membrane resistance by 14%. The data shown in Figure 12 assume a constant membrane thickness, so the changes in the resistivity may represent dimensional changes in the membrane due to applied stresses. At room temperature, the elastic modulus is large, so dimensional changes of the membrane by compression produce only modest changes in the membrane resistance. However, at higher temperatures of 80–100 °C, the modulus is less than 10 MPa, so the applied compression sealing the fuel cell could increase the membrane resistance by factors of 2 or more.

If the hysteresis in the resistivity shown in Figures 12 results from dimensional changes of the membrane, the results from Figure 13 suggest substantial hysteresis in the dimensions of the membrane upon compression and relaxation. According to the compression and relaxation experiment shown in Figure 13, a membrane that is compressed may be frozen into a partially compressed state for extremely long periods of time. The resistance measurements indicate a change of 5% existed between compressing a membrane to 3.6 MPa from 0 MPa and decompressing a membrane to 3.6 MPa from 7.2 MPa.

MEAs for PEM fuel cells are typically made by the pressing of the membrane between the electrodes layers (catalyst and gas diffusion layers) and then by the sealing of the MEA between the bipolar plates that supply the gases to the fuel cell. All this is done while the membrane is dry. In the fuel cell, water is absorbed into the membrane from the feed streams. Membrane hydration is accompanied by membrane swelling. The membrane swelling creates a pressure against the electrode layers and bipolar plates. The swelling pressure of the membrane is the result of the increase in energy by water sorption into the membrane. A simple energy balance shows that the swelling pressure (P_{swelling}) is the energy of water sorption, $\Delta H_{\text{absorption}}$, divided by the change in volume associated with the water sorption $\overline{V}_{H_2O}$.

$$P_{\text{swelling}} = \frac{(\text{Energy of water absorption})}{(\text{Volume change on absorption})} = \frac{[SO_3^-][\#H_2O/SO_3^-][-\Delta H_{\text{absorption}}]}{[SO_3^-][\#H_2O/SO_3^-][\bar{V}_{H_2O}]} \quad (10)$$

Equation 10 is a simple statement that the swelling pressure is the ratio of the enthalpy of water sorption divided by the partial molar volume of water in the membrane. The swelling pressure decreases as the water content increases because the heat of sorption of water decreases with the water content.

Figure 14 shows the dynamic measurement of the swelling pressure of Nafion 115. Just after the water injection, the force increased, went through a maximum 2000 s after water injection, and then relaxed over a time of 50,000 s. The rise in the force after water injection corresponds to the water sorption into the membrane. The dynamic water uptake measurements (Figs. 10 and 11) show that it took 1000–4000 s for water sorption to be equilibrated, which is the same time observed for membrane swelling. The long time relaxation out to 50,000 s is the result of polymer creep from the applied stress of the swelling pressure. The dynamics of the swelling pressure measurement should be representative of what happens in a fuel cell when the membrane is hydrated: it swells, creating a stress, and subsequently creeps because of the applied stress.

The surprising result from the swelling pressure measurements was that the swelling pressure showed little or no dependence on temperature, whereas all the other mechanical properties and water uptake varied substantially with temperature. According to eq 10, the swelling pressure depends on the enthalpy of water absorption and the partial molar volume of water. The enthalpy of water absorption is the solvation energy. By constraining the swelling, we are looking at the water absorption energy for the initially sorbed water, which should correspond to ionization of the acid moieties. The enthalpy of ionization is not very sensitive to temperature. The swelling pressure was used to determine an enthalpy of water sorption of -20 ± 3 kJ/mol. To obtain this value, it was assumed that the partial molar volume of water in Nafion was equal to the molar volume of water. This enthalpy of water absorption is comparable to that obtained by Morris and Sun[12] and by Escoubes and Pineri.[52]

CONCLUSIONS

The mechanical and electrical properties of Nafion and Nafion/TiO_2 composite membranes were examined; we focused on the properties of these materials in constrained environments. The key results from these studies are as follows:

1. Composite membranes have a lower resistivity than Nafion under fully humidified conditions and give better iv performance in fuel cells.
2. Water sorption into Nafion-based membranes increases with increased temperature. Recast membranes sorbed water faster than extruded Nafion.
3. The elastic modulus of dry Nafion and Nafion/TiO_2 composite membranes decreases from 300 MPa at 25 °C to 80 MPa at 90 °C and then decreases to 2–3 MPa at 110 °C.
4. Water sorption is a balance between the energy of solvation of the sulfonic acid groups and the energy to swell the membrane. The reduction of the elastic modulus with increased temperature reduces the energy required to swell the membrane and permits greater water sorption.
5. Water plasticizes Nafion and Nafion/TiO_2 membranes. At room temperature, the elastic modulus decreased from 300 MPa for dry membranes to 50 MPa for fully humidified membranes. The elastic modulus of composite membranes did not decrease as much with the water content as Nafion membranes did.
6. Water reduced the plastic modulus of Nafion/TiO_2 membranes more than that of Nafion.
7. Nafion/TiO_2 membranes crept 40% less than Nafion membranes did at 25 °C and 100% RH after 3 h.

8. The resistance of Nafion and Nafion/TiO_2 membranes increased when they were compressed. The resistance increase was consistent with the elastic compression of the membrane. Increasing and decreasing the compression of the membranes resulted in hysteresis of the resistance. Membranes compressed to the same pressure had different resistance depending on whether the pressure was increased or decreased.
9. Water sorption by Nafion-based membranes results in a swelling pressure. The swelling pressure of a Nafion 115 membrane at 100% RH and 80 °C was 0.55 MPa.
10. The swelling pressure of Nafion was not very sensitive to the temperature. The enthalpy of water absorption into Nafion was −20 kJ/mol on the basis of the swelling pressure.

The results show that the mechanical properties of Nafion-based membranes will impact the dynamic performance of PEM fuel cells, especially during startup when the membranes swell as they absorb water. The results did not reveal any direct connection between the mechanical properties of composite membranes and their improved performance in PEM fuel cells.

The authors thank the National Science Foundation (CTS-0354279 and DMR-0213707 through the Materials Research and Science Engineering Center at Princeton) for its support of this work.

REFERENCES AND NOTES

1. Fuel Cell Systems; Blomen, L. J. M. J.; Mugerwa, M. N., Eds.; Plenum: New York, 1993; p 614.
2. EG&G Services. Fuel Cell Handbook; U.S. Department of Energy: Morgantown, WV, 2000; p 312.
3. Srinivasan, S.; Dave, B. B.; Murugesamoorthi, K. A.; Parthasarathy, A.; Appleby, A. J. In Fuel Cell Systems; Blomen, L. J. M. J.; Mugerwa, M. N., Eds.; Plenum: New York, 1993; pp 37–72.
4. Yang, C.; Costamagna, P.; Srinivasan, S.; Benziger, J.; Bocarsly, A. B. J Power Sources 2001, 103, 1–9.
5. Malhotra, S.; Datta, R. J Electrochem Soc L 1997, 144, 23–26.
6. Doyle, M.; Choi, S.; Proulx, G. J Electrochem Soc 2000, 147, 34–37.
7. Alberti, G.; Casciola, M.; Palombari, R. J Membr Sci 2000, 172, 233–239.
8. Mauritz, K. A.; Payne, J. T. J Membr Sci 2000, 168, 39–51.
9. Gebel, G.; Aldebert, P.; Pineri, M. Polymer 1993, 34, 333–339.
10. Kreuer, K. D. J Membr Sci 2001, 185, 29–39.
11. Choi, P.; Jalani, N. H.; Datta, R. J Electrochem Soc E 2005, 152, 84–89.
12. Morris, D. R.; Sun, X. D. J Appl Polym Sci 1993, 50, 1445–1452.
13. Chen, S. L.; Bocarsly, A. B.; Benziger, J. J Power Sources 2005, 152, 27–33.
14. Aldebert, P.; Guglielmi, M.; Pineri, M. Polym J 1991, 23, 399–406.
15. Benziger, J.; Chia, E.; Moxley, J. F.; Kevrekidis, I. G. Chem Eng Sci 2005, 60, 1743–1759.
16. Escoubes, M.; Pineri, M.; Robens, E. Thermochim Acta 1984, 82, 149–160.
17. Bauer, F.; Denneler, S.; Willert-Porada, M. J Polym Sci Part B: Polym Phys 2005, 43, 786–795.
18. Pineri, M. ACS Symp Ser 1986, 302, 159–174.
19. Jalani, N. H.; Datta, R. J Membr Sci 2005, 264, 167–175.
20. Yeo, S. C.; Eisenberg, A. J Appl Polym Sci 1977, 21, 875–898.
21. Hinatsu, J. T.; Mizuhata, M.; Takenaka, H. J Electrochem Soc 1994, 141, 1493–1498.
22. Zook, L. A.; Leddy, J. Anal Chem 1996, 68, 3793–3796.
23. Lee, W. K.; Ho, C. H.; Van Zee, J. W.; Murthy, M. J Power Sources 1999, 84, 45–51.
24. Adjemian, K. T.; Lee, S. J.; Srinivasan, S.; Benziger, J.; Bocarsly, A. B. J Electrochem Soc A 2002, 149, 256–261.
25. Antonucci, P. L.; Arico, A. S.; Creti, P.; Ramunni, E.; Antonucci, V. Solid State Ionics 1999, 125, 431–437.
26. Doyle, M.; Choi, S.; Proulx, G. J Electrochem Soc 2000, 147, 34–37.
27. Grot, W. G.; Rajendran, G. Membranes Containing Inorganic Fillers and Membrane and Electrode Assemblies and Electrochemical Cells Employing Same; United States, US Patent No 5919583, July 6, 1999.
28. Honma, I.; Hirakawa, S.; Yamada, K.; Bae, J. M. Solid State Ionics 1999, 118, 29–36.
29. Lee, S. J.; et al. The Electrochemical Society Meeting; Electrochemical Society: Toronto, Canada, 2000.
30. Malhotra, S.; Datta, R. J Electrochem Soc L 1997, 144, 23–26.
31. Mauritz, K. A. Mater Sci Eng 1998, 6, 121–133.
32. Miyake, N.; Wainright, J. S.; Savinell, R. F. J Electrochem Soc A 2001, 148, 898–904.
33. Murphy, O. J.; Cisar, A. J. Composite Membrane Suitable for Use in Electrochemical Devices; United States, Patent No 6,059,943; May 9, 2000.
34. Si, Y.; Lin, J.-C.; Kunz, H. R.; Fenton, J. M. Meeting of the Electrochemical Society; Electrochemical Society: Philadelphia, 2002.
35. Honma, I.; Nishikawa, O.; Sugimoto, T.; Nomura, S.; Nakajima, H. Fuel Cells 2002, 2, 52–58.
36. Adjemian, K. T.; Srinivasan, S.; Benziger, J.; Bocarsly, A. B. J Power Sources 2002, 109, 356–364.

37. Chen, T.-Y.; Leddy, J. Langmuir 2000, 16, 2866–2871.
38. Clearfield, A.; Stynes, J. A. J Inorg Nucl Chem 1964, 26, 117–129.
39. Zawodzinski, T. A.; Derovin, C. R.; Radzinski, S.; Sherman, R. J.; Smith, V. T.; Springer, T. E.; Gottesfeld, S. J Electrochem Soc 1993, 140, 1041–1047.
40. Choi, P. H.; Datta, R. J Electrochem Soc E 2003, 150, 601–607.
41. Alfrey, T. J.; Gurnee, E. F. Organic Polymers; Prentice Hall: Englewood Cliffs, NJ, 1967.
42. Loveday, D.; Wilkes, G. L.; Lee, Y.; Storey, R. F. J Appl Polym Sci 1997, 63, 507–519.
43. Jalani, N. H.; Dunn, K.; Datta, R. Electrochim Acta 2005, 51, 553–560.
44. Wood, L. A.; Bullman, G. W. J Polym Sci Part A-2: Polym Phys 1972, 10, 43–50.
45. Publishing, W. A. Effect of Creep and Other Time Related Factors on Plastics and Elastomers; Plastic Design Library; William Anderson Publishing: Norwich, NY; 1991.
46. Mauritz, K. A.; Moore, R. B. Chem Rev 2004, 104, 4535–4585.
47. Bunce, N. J.; Sondheimer, S. J.; Fyfe, C. A. Macromolecules 1986, 19, 333–339.
48. Alberti, G.; Casciola, M.; Massinelli, L.; Bauer, B. J Membr Sci 2001, 185, 73–81.
49. Zawodzinski, T. A.; Springer, T. E.; Davey, J.; Jestel, R.; Lopez, C.; Valerio, J.; Gottesfeld, S. J Electrochem Soc 1993, 140, 1981–1985.
50. Yang, C.; Srinivasan, S.; Bocarsly, A. B.; Tulyani, S.; Benziger, J. B. J Membr Sci 2004, 237, 145– 161.
51. Jalani, N. H.; Choi, P.; Datta, R. J Membr Sci 2005, 254, 31–38.
52. Escoubes, M.; Pineri, M. ACS Symp Ser 1982, 180, 9–23.